AIAA JOURNAL
Vol. 45, No. 5, May 2007

Aeroelastic Analysis of an Isolated Airfoil Under a Pulsating Flow

Seung Ho Cho*
Seoul National University, Seoul 151-742, Republic of Korea
Taehyoun Kim†
Boeing Commercial Airplane Company, Seattle, Washington 98124-2207
and
Seung Jin Song‡ and Sang Joon Shin§
Seoul National University, Seoul 151-742, Republic of Korea

DOI: 10.2514/1.25485

Significant progress has been made in aeroelastic analysis of an isolated airfoil, mostly under the assumption of a steady freestream. In reality, however, the inflowing freestream is often pulsating. Therefore, this paper presents a stability analysis of an isolated airfoil under pulsating freestream conditions and a forced response analysis of an isolated rotor blade rotating at a constant angular velocity. First, a new unsteady vortex lattice model with an unsteady freestream flow has been developed in discrete time domain to examine unsteady aerodynamic forces acting on a vibrating airfoil. Second, the airfoil's aeroelastic behavior has been analyzed using a typical section method. The 2-D analysis requires a structural dynamic solution coupled with aerodynamic calculation. In the aeroelastic analysis, the flutter onset of an airfoil under pulsating freestream is predicted using Floquet analysis. Finally, the forced response of a rotating airfoil due to a combination of a time-varying angle of attack and a time-varying freestream has been examined.

Nomenclature

b	=	half chord of airfoil
e	=	distance from the midchord to the elastic axis
F	=	unsteady aerodynamic load vector
h	=	vertical displacement
I_α	=	moment of inertia
i	=	index number of collocation point
j	=	index number of vortex
K	=	kernel function; stiffness matrix
L	=	unsteady lift
L_0	=	steady lift
M	=	mass matrix; total number of bound vortex elements
M_{EA}	=	unsteady moment about the elastic axis
m	=	mass
N	=	total number of vortex elements
n	=	time level
Q	=	Floquet transition matrix
q	=	state vector of airfoil
R_α	=	radius of gyration
S	=	surface area
T	=	period
t	=	time
U	=	freestream velocity
U_∞	=	mean freestream velocity
$\bar{u}$	=	magnitude of stream pulsations
V	=	rotational speed of rotor
w	=	downwash velocity
w_g	=	downwash due to incident vertical gust
x	=	location of collocation point
x_α	=	static imbalance
α	=	weighting factor; angle of attack
Γ	=	vortex strength
γ	=	vorticity per unit length
μ	=	mass ratio
ξ	=	location of vortex
ρ	=	air density
τ	=	nondimensional time
Ω	=	frequency of stream pulsations
ω	=	decoupled frequency

Subscripts

h	=	plunging
α	=	pitching
1	=	on airfoil
2	=	in wake

Presented as Paper 1968 at the 47th AIAA/ASME/ASCE/AHS/ASC Structures, Structural Dynamics and Materials Conference, Newport, RI, 1–4 May 2006; received 28 May 2006; revision received 11 December 2006; accepted for publication 2 January 2007.

*Research Assistant, School of Mechanical and Aerospace Engineering.
†Principal Engineer, Loads and Dynamics. Member AIAA.
‡Associate Professor, School of Mechanical and Aerospace Engineering.
§Assistant Professor, Institute of Advanced Aerospace Technology, School of Mechanical and Aerospace Engineering. Member AIAA.

I. Introduction

AEROLASTIC analysis is needed to examine the forced and self-excited (i.e., flutter) response of aircraft wings or turbomachinery blades. In turn, aeroelastic analysis requires a coupling between unsteady aerodynamics and structural dynamics. The modeling of unsteady aerodynamics can be conducted in either frequency or time domain. Often, aeroelastic stability analysis is carried out in the frequency domain (e.g., V–g method and p–k method). In the frequency domain, the flow unsteadiness is assumed to be a small harmonic (i.e., $e^{i\omega t}$) perturbation about the mean flow. Using such methods, Ehlers and Weatherill [1] and Whitehead [2,3] calculated unsteady aerodynamic forces acting on an isolated airfoil and a cascade, respectively.

On the other hand, a time-domain analysis can give information regarding the temporal evolution of aerodynamic and structural behavior. To obtain time-domain models, unsteady aerodynamic forces in the frequency domain have been formulated as an approximate rational function using the Laplace transform

techniques [4,5], resulting in an aeroelastic model with augmented aerodynamic states. To obtain aerodynamic models directly in the time domain, Hall has proposed a reduced-order model for unsteady aerodynamic forces in airfoils, cascades, and wings [6]. Kim et al. extended the method to continuous time domain, and eliminated the bound vortex using a static condensation [7]. However, such analyses have been limited to time-invariant, steady freestream inflow conditions.

Fundamental solutions for an oscillating airfoil under a steady flow have been given in closed form by Theodorsen [8], and in operational form by Sears [9]. To the authors' best knowledge, the first attempt to derive a closed-form solution for pulsating freestream conditions has been conducted by Isaacs [10]. At about the same time, Greenberg has extended Theodorsen's theory to include pulsating freestream conditions [11]. Later, van der Wall and Leishman have solved the problem of the periodic coefficients by a transformation from the time variable to a space variable [12,13], and Peters et al. show how the state-space equations yield periodic-coefficient equations in rotorcraft applications [14,15]. In the field of turbomachinery, Dugundji and Bundas have calculated unsteady aerodynamic forces on a rotating blade row under nonuniform inflow conditions to investigate a cascade's forced response. In their case, the flow nonuniformity in the absolute frame results in unsteady freestream conditions for rotating blades. They assume a small nonuniformity and do not account for its influence on stability [16]. In spite of such efforts, the effects of arbitrary magnitudes and frequencies of freestream pulsations on aerodynamics and airfoil stability still remain unknown.

To address such issues, this paper presents a new analytical model. A new unsteady aerodynamic model, consisting of a vortex lattice model, for an isolated airfoil in a pulsating freestream is first presented. Subsequently, the airfoil's stability under pulsating freestream flow conditions is discussed. Finally, the forced response of an isolated rotating blade under nonuniform freestream is examined.

II. Model Description

A. Unsteady Aerodynamic Model

The unsteady aerodynamic forces on an isolated airfoil have been calculated using a new 2-D unsteady vortex lattice method (Fig. 1). The vortices have been divided into bound and free vortices; the former is located on the airfoil and the latter in the trailing wake. Point vortices are located on the airfoil and in the wake at the quarter chord of the total of N panels. The downwash due to the vortices w_i^n is computed on the airfoil at the three-quarter chord of M locations:

$$w^n = \begin{bmatrix} K_1 & K_2^n \end{bmatrix} \begin{Bmatrix} \Gamma_1^n \\ \Gamma_2^n \end{Bmatrix} \tag{1}$$

The downwash w_i^n is a $(M \times 1)$ vector containing the downwash at time step n, and it is affected by incident vertical gusts as well as motion of the airfoil itself. Γ_1^n and Γ_2^n are the strengths of the airfoil and wake vortices at time step n, respectively. For an isolated flat plate in 2-D incompressible flow, the kernel function is [17]

$$K_{ij} = \frac{1}{2\pi(x_i - \xi_j)} \qquad (i = 1, \ldots, M; j = 1, \ldots, N) \tag{2}$$

where x_i is the location of the ith collocation point, and ξ_j is the location of the jth vortex. In a pulsating flow, the location of the bound vortex, ξ_j $(j = 1, \ldots, M)$, is time-invariant because the vortex elements can be assumed to be of equal size Δx on the airfoil. However, the location of the wake vortex, $\xi_j(t)(j = M + 1, \ldots, N)$, is time-varying because the elemental length changes according to $\Delta x(t) = U(t)\Delta t$. Thus, the location of the wake vortex is

$$\xi_j(t) = \int_{(n+M-j)\Delta t}^{n\Delta t} U(t)\,\mathrm{d}t \qquad (j = M + 1, \ldots, N) \tag{3}$$

where the freestream velocity $U(t)$ is arbitrarily time-varying.

For this investigation, the freestream velocity is assumed to be sinusoidal:

$$U(t) = U_\infty + \bar{u}\cos\Omega t \tag{4}$$

The conservation of the vorticity dictates that

$$\Gamma_{M+1}^{n+1} = -\sum_{j=1}^{M}\left(\Gamma_j^{n+1} - \Gamma_j^n\right) \tag{5}$$

For convection of free wakes with speed $U(t)$ in discrete time domain,

$$\Gamma_j^{n+1} = \Gamma_{j-1}^n \qquad (j = M + 2, \ldots, N - 1) \tag{6}$$

$$\Gamma_N^{n+1} = \alpha\Gamma_N^n + \Gamma_{N-1}^n \qquad (0.95 < \alpha < 1) \tag{7}$$

With the weighting factor α in Eq. (7) one can cut off the infinitely long wake vortex at a finite length. For an isolated airfoil under steady flow, Hall has suggested $0.95 < \alpha < 1$ [6].

Combining the kernel function equation [Eq. (1)], the vorticity conservation equation [Eq. (5)], and the equations for the convection of free wakes [Eqs. (6) and (7)], the aerodynamic equations can be expressed as

$$\begin{bmatrix} O & O \\ A_1 & A_2 \end{bmatrix} \begin{Bmatrix} \Gamma_1 \\ \Gamma_2 \end{Bmatrix}^{n+1} = \begin{bmatrix} K_1 & K_2 \\ B_1 & B_2 \end{bmatrix} \begin{Bmatrix} \Gamma_1 \\ \Gamma_2 \end{Bmatrix}^{n} - \begin{Bmatrix} w \\ O \end{Bmatrix}^{n} \tag{8}$$

To reduce the size of the equation, the bound vortex Γ_1^n is eliminated by using static condensation as follows [7]: Solving for Γ_1^n from the kernel function, Eq. (1) gives

$$\Gamma_1^n = -K_1^{-1}K_2^n\Gamma_2^n + K_1^{-1}w^n \tag{9}$$

Equation (9) is then substituted into Eq. (8) to give

$$\Gamma_2^{n+1} = \left(-A_1K_1^{-1}K_2^{n+1} + A_2\right)^{-1}\Big[\left(-B_1K_1^{-1}K_2^n + B_2\right)\Gamma_2^n - A_1K_1^{-1}w^{n+1} + B_1K_1^{-1}w^n\Big] \tag{10}$$

The unsteady lift and moment about the elastic axis can be obtained as [6]

$$L = \int_{-b}^{b}\rho\left[U\gamma(x) + \frac{\mathrm{d}}{\mathrm{d}t}\int_{-b}^{x}\gamma(x_1)\,\mathrm{d}x_1\right]\mathrm{d}x \tag{11}$$

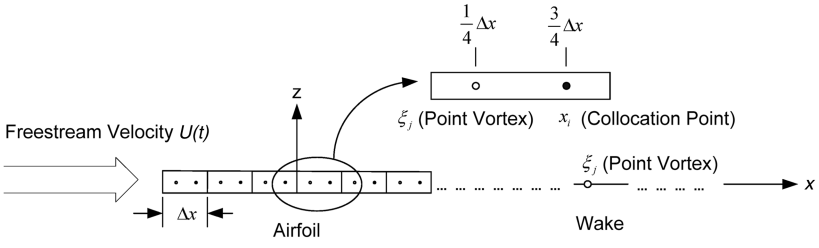

Fig. 1 Discrete vortex model for a 2-D airfoil.

$$M_{\mathrm{EA}} = \int_{-b}^{b} \rho(x-e)\left[U\gamma(x) + \frac{\mathrm{d}}{\mathrm{d}t}\int_{-b}^{x} \gamma(x_1)\,\mathrm{d}x_1\right]\mathrm{d}x \tag{12}$$

where the freestream velocity U is time-varying, and γ, ρ, e, and b are the vorticity per unit length, the density, the distance from the midchord to the elastic axis, and the half chord of the airfoil, respectively. Discretization of Eqs. (11) and (12) gives the unsteady lift and moment acting on the airfoil as follows:

$$L^n = \rho U(t)\sum_{j=1}^{M}\Gamma_j^n + \rho\sum_{j=1}^{M}\sum_{k=1}^{j}\dot{\Gamma}_k^n\Delta x_j \tag{13}$$

$$M_{\mathrm{EA}}^n = \rho U(t)\sum_{j=1}^{M}(\xi_j - e)\Gamma_j^n + \rho\sum_{j=1}^{M}(\xi_j - e)\sum_{k=1}^{j}\dot{\Gamma}_k^n\Delta x_j \tag{14}$$

B. Aeroelastic Model

To model an aeroelastic system, the unsteady aerodynamic model is coupled with a structural dynamic model of a typical section of the airfoil (Fig. 2). The equations of motion in plunging and pitching in continuous time domain are [7]

$$\begin{bmatrix} m & mx_\alpha b \\ mx_\alpha b & I_\alpha \end{bmatrix}\begin{Bmatrix} \ddot{h} \\ \ddot{\alpha} \end{Bmatrix} + \begin{bmatrix} K_h & 0 \\ 0 & K_\alpha \end{bmatrix}\begin{Bmatrix} h \\ \alpha \end{Bmatrix} = \begin{Bmatrix} -LS \\ M_{\mathrm{EA}}S \end{Bmatrix} \tag{15}$$

where the typical section has mass m, moment of inertia I_α, bending stiffness K_h, torsional stiffness K_α, distance from midchord to elastic axis x_α, and surface area S. The plunging displacement h is positive downward, and the pitching angle α is positive nose-up. A nondimensional form of Eq. (15) is

$$\begin{bmatrix} 1/\bar{R}_\alpha^2 & x_\alpha/\bar{R}_\alpha^2 \\ x_\alpha/\bar{R}_\alpha^2 & 1 \end{bmatrix}\begin{Bmatrix} \ddot{\bar{h}} \\ \ddot{\alpha} \end{Bmatrix} + \begin{bmatrix} \bar{\omega}_h^2/\bar{R}_\alpha^2 & 0 \\ 0 & 1 \end{bmatrix}\begin{Bmatrix} \bar{h} \\ \alpha \end{Bmatrix} = \begin{Bmatrix} -LSb/K_\alpha \\ M_{\mathrm{EA}}S/K_\alpha \end{Bmatrix} \tag{16}$$

where $(\cdot)$ denotes a derivative with respect to the nondimensional time τ, and

$$\tau = \omega_\alpha t, \qquad R_\alpha = \sqrt{I_\alpha/m}, \qquad \bar{R}_\alpha = R_\alpha/b, \qquad \bar{h}_\alpha = h/b$$
$$\bar{\omega}_h = \omega_h/\omega_\alpha, \qquad \omega_h = \sqrt{K_h/m}, \qquad \omega_\alpha = \sqrt{K_\alpha/I_\alpha} \tag{17}$$

For simplicity, Eq. (16) is expressed as

$$M\begin{Bmatrix} \ddot{\bar{h}} \\ \ddot{\alpha} \end{Bmatrix} + K\begin{Bmatrix} \bar{h} \\ \alpha \end{Bmatrix} = F \tag{18}$$

Converting Eq. (18) into a state-space form in the continuous time domain gives [18]

$$\dot{q} = \begin{bmatrix} O & I \\ -M^{-1}K & O \end{bmatrix}q + \begin{bmatrix} O \\ M^{-1} \end{bmatrix}F \tag{19}$$

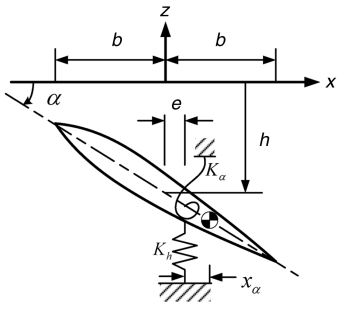

Fig. 2 Typical section model with two degrees of freedom.

where the state vector of the airfoil, q, is $[h \quad \alpha \quad \dot{h} \quad \dot{\alpha}]^T$. Discretizing Eq. (19) in time, a discrete time-domain form is obtained as follows:

$$q^{n+1} = A_s q^n + B_s F^n \tag{20}$$

The downwash vector is related to incident vertical gusts and the state vector of the airfoil as

$$w^n = w_g^n + E^n q^n \tag{21}$$

Combining Eqs. (10), (13), (14), (20), and (21), the following contracted aeroelastic equations of motion are obtained:

$$\begin{bmatrix} A & E \\ C_2 & D_2 \end{bmatrix}\begin{Bmatrix} \Gamma_2 \\ q \end{Bmatrix}^{n+1} = \begin{bmatrix} B & O \\ C_1 & D_1 \end{bmatrix}\begin{Bmatrix} \Gamma_2 \\ q \end{Bmatrix}^{n} - \begin{Bmatrix} w_g \\ O \end{Bmatrix}^{n} \tag{22}$$

C. Floquet Analysis

Because the matrices A and B in Eq. (22) are periodic functions of time, their stability cannot be directly determined by standard eigenvalue analysis. A common stability analysis for periodic systems is the calculation of time histories of responses with respect to initial disturbances [19]. However, this method is cumbersome and does not produce clear answers when the system is nearly neutrally stable. Therefore, Floquet analysis has been used in this paper, and the Floquet transition matrix, which relates the state variables at the beginning and end of one period, has been obtained [20]. Then, the dynamic stability of the periodic system can be determined from the eigenvalues of this matrix.

The periodic aeroelastic equation [Eq. (22)] may be written as

$$\begin{Bmatrix} \Gamma_2 \\ q \end{Bmatrix}^{n+1} = [D(n)]\begin{Bmatrix} \Gamma_2 \\ q \end{Bmatrix}^{n} + \{G(n)\} \tag{23}$$

where $D(n)$ is periodic with period T. If the freestream velocity is assumed to be sinusoidal [Eq. (4)], the period is determined by the frequency of stream pulsations ($T = 2\pi/\Omega$). Then, the stability of the system is taken to be identical with the stability of the transient solutions to Eq. (23).

The Floquet transition matrix Q of the system is defined by

$$\begin{Bmatrix} \Gamma_2 \\ q \end{Bmatrix}^{t=T} = [Q]\begin{Bmatrix} \Gamma_2 \\ q \end{Bmatrix}^{t=0} \tag{24}$$

for all sets of initial conditions $[\Gamma_2 \quad q]^{T\,t=0}$ applied to Eq. (23) with $G(n) = 0$. The eigenvalues of Q determine the dynamic stability of the periodic aeroelastic system. If any of the eigenvalues has a magnitude greater than unity, the system is unstable.

III. Model Predictions

A. Unsteady Aerodynamic Results

This section presents validation results of the new unsteady vortex lattice model under a steady inflow as well as a pulsating freestream. The input parameters of the model for steady inflow are based on Hall's work [6], and those for a pulsating flow on Isaacs's work [10] (Table 1). First, Wagner's problem of a step change in the angle of attack under a steady flow has been analyzed, and Fig. 3 shows the calculated unsteady lift under such conditions. For this case, the magnitude of freestream pulsations $\bar{u}$ has been set to zero. This new vortex lattice method result matches the Wagner's function well [21].

Table 1 Aerodynamic parameters of an isolated airfoil

Parameter	Value
Vortex elements of airfoil	20
Vortex elements of wake	200
Weighting factor	0.996
$\Omega b/U_\infty$	0.0424
$\bar{u}/U_\infty$	0.0 (steady flow), 0.4 (pulsating flow)

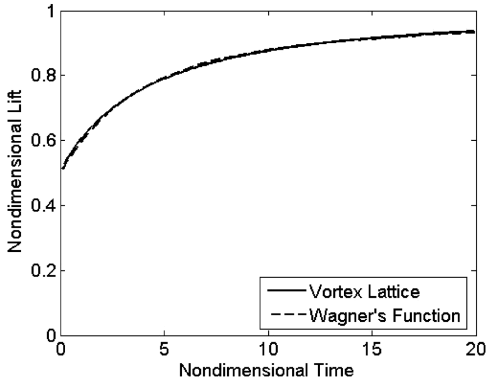

Fig. 3 Indicial lift under steady flow due to a step input in vortex lattice method and Wagner's function field.

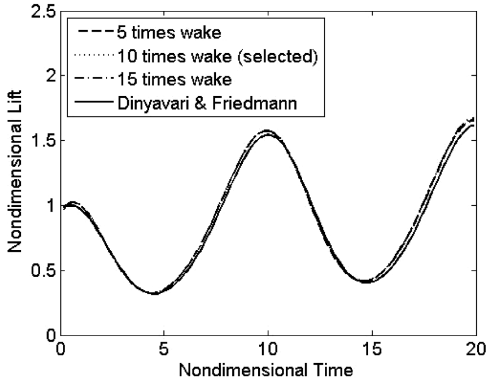

Fig. 4 Indicial lift under pulsating flow due to a step input in vortex lattice method with three different wake lengths, and Dinyavari and Friedmann's result for $\bar{u}/U_\infty = 0.4$ [5].

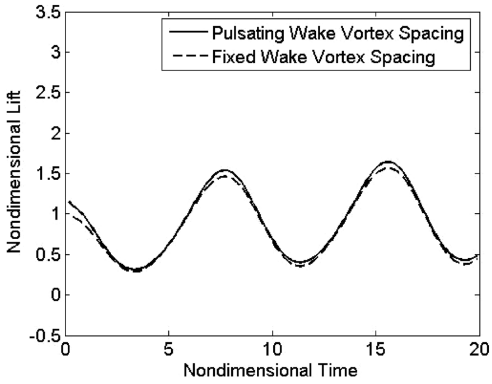

Fig. 5 Indicial lift under pulsating flow due to a step input with pulsating and fixed wake vortex spacing when the magnitude of stream pulsations is 40% of mean freestream velocity.

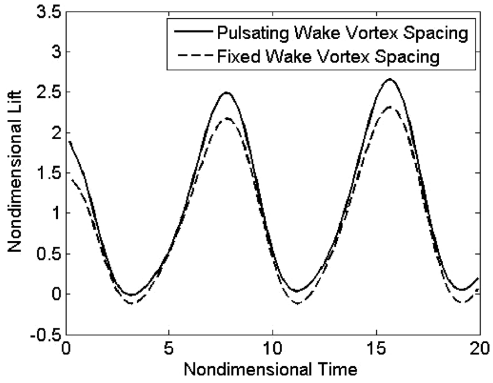

Fig. 6 Indicial lift under pulsating flow due to a step input with pulsating and fixed wake vortex spacing when the magnitude of stream pulsations is 80% of mean freestream velocity.

Figure 4 illustrates the time history of the calculated unsteady lift under a pulsating stream with three different wake lengths when the airfoil is forced to pitch suddenly in the step function at the nondimensional time $\tau = 0$. Here, the unsteady lift is normalized by the steady-state lift. The wake sheets are, respectively, 5, 10, and 15 times longer than the airfoil chord. This figure shows that the results under pulsating inflow are not very sensitive to the length of the free wake, and placing vortex elements on the wake 10 times more than on the chord is sufficient for the analysis under pulsating inflows. Hence, for all the results that follow the wake length was set to be 10 times the chord as listed in Table 1. Also shown in Fig. 4 for comparison is Dinyavari and Friedmann's result [5], which is the time-domain version of Greenberg's theory [11]. The results from the new vortex lattice model agree well with Dinyavari and Friedmann's result. After sufficient time has passed, the unsteady lift from the new model matches Greenberg's value, which is the steady-state solution obtained from the frequency domain analysis. For nondimensional time less than about 10, transient effects, which can be captured only with the time-domain analysis, are visible.

Greenberg [11] has assumed fixed wake vortex spacing in his unsteady analysis and used the mean freestream velocity to define the position of the vortices in the airfoil wake. The new model, which incorporates time-varying wake vortex spacing, has been used to test this assumption (Figs. 5–7). A nondimensional velocity fluctuation amplitude $\bar{u}/U_\infty$ is defined as the ratio of magnitude of stream pulsations to mean freestream velocity. Figure 5 shows unsteady lift under a pulsating flow with pulsating and fixed wake vortex spacing for $\bar{u}/U_\infty = 0.4$, which is based on Isaacs's work [10]. Figure 6 shows the corresponding results for $\bar{u}/U_\infty = 0.8$. Figure 5 shows that the effects of the pulsating wake vortex spacing may be neglected when the nondimensional velocity fluctuation amplitude is 0.4. However, the difference between the magnitudes of the lift of the pulsating and the fixed wake vortex spacing solutions becomes significant as the nondimensional velocity fluctuation amplitude increases (Fig. 6). On the other hand, the differences in the phase of the lift remain insignificant.

Figure 7 shows the ratios of the lift (maximum lift, lift deviation, and mean lift) with pulsating wake vortex spacing and the lift with fixed wake vortex spacing plotted vs nondimensional velocity fluctuation amplitude. The maximum lift, lift deviation, and mean lift are important for determining the cracking, fatigue loading, and endurance limits of airfoils, respectively. The difference between the maximum lift with the pulsating wake vortex spacing and that with fixed wake vortex spacing becomes significant above $\bar{u}/U_\infty = 0.41$. For the lift deviation and mean lift, the differences become significant above $\bar{u}/U_\infty = 0.63$ and 0.35, respectively. Therefore, the validity of fixed wake vortex spacing depends on the type of problem under question. For example, the assumption of the fixed wake vortex spacing might not be accurate for $\bar{u}/U_\infty > 0.4$ for fatigue.

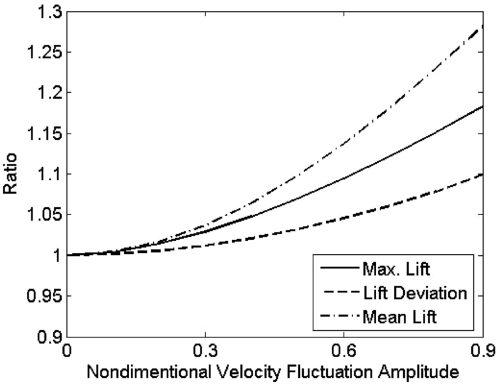

Fig. 7 Lift (maximum, deviation, and mean) ratios of pulsating and fixed wake vortex spacing.

Table 2 Structural parameters of the typical section [6,7]

Parameter	Value
x_α/b	0.2
ω_h/ω_α	0.3
R_α/b	0.5
μ	20.0
e/b	−0.1

Table 3 Flutter speed under a steady flow

Analysis	Flutter speed
V–g analysis	2.0
Eigenmode analysis in discrete time domain [6]	2.0
Eigenmode analysis in continuous time domain [7]	2.0
Floquet analysis	1.9

B. Aeroelastic Stability Results

A typical section model used in this paper is shown in Fig. 2. This model has two degrees of freedom: plunge h and pitch α. Linear and torsional springs at the elastic axis act to restrain motion in bending and torsion, respectively. Shown in Table 2 are the structural parameters of the typical section model used in this paper. These values for typical section are based on Hall's work [6].

The mean freestream velocity U_∞ at which the aeroelastic system becomes unstable is called the time-averaged flutter speed. Table 3 lists the flutter speeds predicted by the new unsteady vortex lattice model under a steady flow. Predicted flutter speeds from other methods have also been listed for comparison. In the V–g analysis, the unsteady aerodynamics formulated by Theodorsen [8] is used. In Floquet analysis, the magnitude of stream pulsations, $\bar{u}$ has been assumed to be zero. The value of 1.9 obtained from the new vortex lattice model agrees with the value of 2.0 predicted by other methods. The small difference is due to the time integration in Floquet analysis.

The stability of aeroelastic system changes as the nondimensional magnitude $\bar{u}\omega_\alpha/b$ is varied. Figure 8 shows the time-averaged flutter speed plotted vs the magnitude of stream pulsations when the frequency of stream pulsations has been fixed to be $\pi/10$. The time-averaged flutter speed decreases monotonically as the magnitude of stream pulsations is increased. Thus, increasing magnitude of stream pulsation destabilizes the aeroelastic system at this pulsation frequency.

C. Nonclassical Stability Boundary: Parametric and Combinatory Resonances

Figure 9 shows the flutter boundary of stream pulsations for three different mean freestream velocities. The regions above the boundary lines are unstable, whereas the regions below the boundary are stable. At $U_\infty = 1.8$, two valleys exist. One is between the frequencies of stream pulsations 0.7 and 0.75, and the other is between 0.8 and 0.85. The undamped natural frequencies of the 2-D airfoil are 0.298 (plunging) and 1.10 (pitching) rad/s in the current case (Table 2). The valley between 0.7 and 0.75 seems to be near a parametric resonance because one parametric resonance frequency is $2 \times 1.10/3 = 0.73$. On the other hand, the valley between 0.8 and 0.85 seems to be near a combinatory resonance frequency of $1.10 - 0.298 = 0.802$. Strictly speaking, the classical parametric and combinatory resonances are defined only for linear (i.e., undamped) periodic systems [22]. Hence, they are not applicable to this system, which has nonzero damping terms and higher harmonic terms. Nevertheless, Fig. 9 shows that phenomena similar to the two types of resonance occur in the current system. Asymptotically, these flutter boundaries approach their steady values under a steady flow as the frequency of stream pulsations goes to zero. Figure 9 shows that even at mean freestream velocities well below the steady freestream flutter speed of 1.9, instabilities can still occur depending on the magnitude and frequency of stream pulsations. Furthermore, several of the instabilities resembling the parametric and combinatory resonances occur at very low pulsating magnitudes leading to potentially dangerous flow situations. The locations of valleys change for different mean freestream velocities because system characteristics including its fundamental eigenvalues change as functions of the freestream velocity.

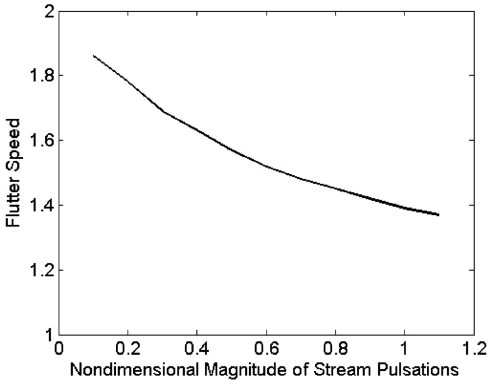

Fig. 8 Flutter speed as a function of the nondimensional magnitude of stream pulsations when the frequency of stream pulsations is fixed to be $\pi/10$.

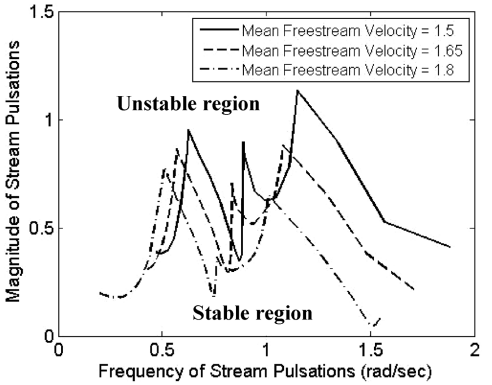

Fig. 9 Flutter boundary of stream pulsations for three different mean freestream velocities.

D. Forced Response of a Rotating Airfoil Under a Pulsating Freestream

Consider an isolated rotor blade on a rigid disk, which is rotating at a constant speed V (Fig. 10). The time-varying pulsation in the absolute incoming velocity, coupled with a constant rotational speed, results in a time-varying angle of attack as well as a time-varying

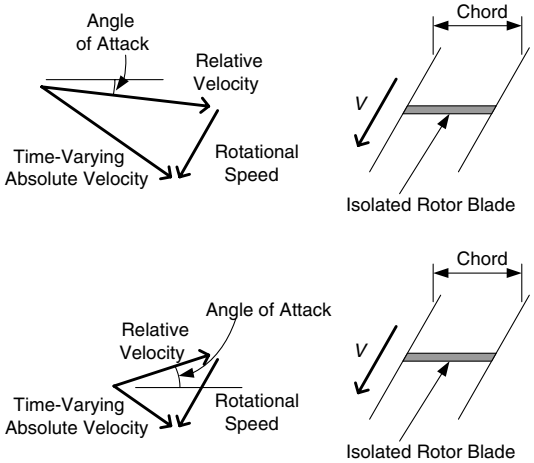

Fig. 10 Rotor geometry and velocity triangle considering rotational speed and time-varying absolute velocity (upper: high velocity case, lower: low velocity case).

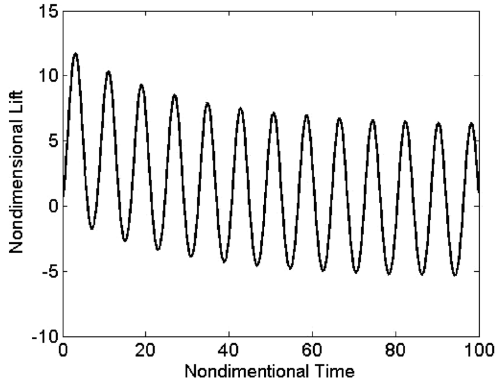

Fig. 11 Transient lift due to pulsating flow with rotational speed for $\bar{u}/U_\infty = 0.4$.

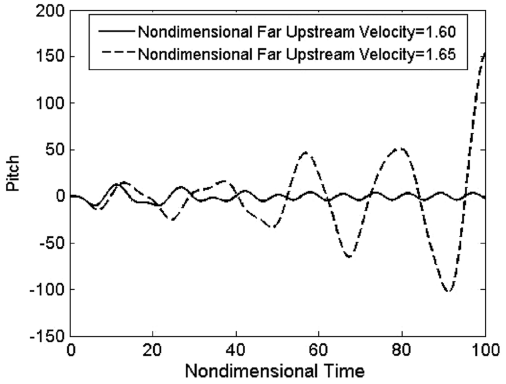

Fig. 13 Transient pitch response due to pulsating flow with rotational speed for $\bar{u}/U_\infty = 0.4$.

relative velocity. Because the homogeneous solution of the aeroelastic equations [Eq. (22)] determines the flutter characteristics, the rotor blade's flutter characteristics remain unchanged. However, the time-varying angle of attack leads to a forced response of the rotor blade, which is given by the nonhomogeneous solution of the same equations. Though Dugundji and Bundas have investigated this issue [16], they solve an arbitrarily transient motion by fitting the sinusoidal aerodynamic coefficients of Whitehead's frequency domain model using Pade approximation, ignoring the effects of the freestream pulsations on the homogeneous part of the equations [14]. However, in this paper, such forced response has been analyzed directly in the time domain using the newly developed model.

Figure 11 shows the transient lift when the steady freestream is suddenly changed into a pulsating freestream with a nondimensional velocity fluctuation amplitude of $\bar{u}/U_\infty = 0.4$ at $\tau = 0$ with the pulsating frequency set equal to $\tau/10$. The design flow coefficient has been set to 0.5 because it is representative of modern turbomachinery. Because most airfoils stall at incidence angles above 10 deg, the nondimensional velocity fluctuation amplitude $\bar{u}/U_\infty$ has been kept below 0.4 to avoid stall. The transient effect disappears after $\tau \approx 80$, as shown in Fig. 11. The transient effect is further limited by aerodynamic damping. The unsteady lift becomes sinusoidal due to the pulsating angle of attack as well as the pulsating relative velocity. Thus, fatigue problems may occur due to the pulsating lift.

Figures 12 and 13 show the transient plunge and pitch, respectively, when the steady freestream is suddenly changed into a pulsating freestream with $\bar{u}/U_\infty = 0.4$ at $\tau = 0$. These responses are obtained for two different mean freestream speeds: one below and another above the flutter speed. Again, the flow coefficient U_∞/V has been assumed to be 0.5. Although forced vibration exists, flutter has not yet occurred at a nondimensional upstream relative velocity of 1.6. However, flutter has already begun at a nondimensional upstream relative velocity of 1.65, and the forced response diverges above the flutter speed. Thus, the time-averaged flutter speed, which corresponds to the relative velocity in Fig. 10, has been calculated to be 1.63. Like a fixed airfoil, when subjected to a pulsating freestream, a rotating blade can flutter below the steady freestream flutter speed of 1.9.

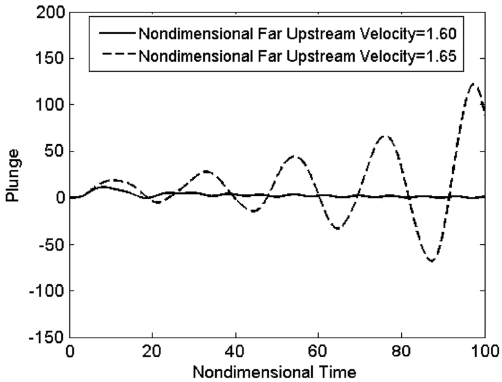

Fig. 12 Transient plunge response due to pulsating flow with rotational speed for $\bar{u}/U_\infty = 0.4$.

IV. Conclusions

The new conclusions of this paper can be summarized as follows:

1) A new vortex lattice model has been developed to analyze a) the aeroelastic stability of an isolated airfoil under pulsating freestream conditions, and b) the forced response of an isolated blade rotating at a constant angular velocity.

2) From the aerodynamic point of view, the assumption of the fixed wake vortex spacing becomes less valid with increasing $\bar{u}/U_\infty$ due to the differences in the maximum and mean lift.

3) Because of pulsations in the freestream, a flutter instability can occur at a mean flow speed lower than the steady flutter speed.

4) In a pulsating freestream, increasing magnitude of stream pulsations decreases the time-averaged flutter speed and destabilizes the aeroelastic system.

5) However, when resonances similar to the classical parametric and combinatory resonances occur, the relationship can be reversed. Near the resonance frequency, ever a small perturbation in the pulsation can trigger the aeroelastic instability.

6) In a rotating blade, a forced response in addition to flutter occurs due to the time-varying angle of attack.

The new formulation could also be useful for analyzing aerodynamic and aeroelastic behavior of an airfoil in a highly unsteady flow field where the time-varying inflow speed is not necessarily periodic but arbitrary.

Acknowledgments

The following financial support from the Korean government is gratefully acknowledged: the BK21 Program of the Ministry of Education and Human Resources Development, the Basic Research Fund of the Korea Research Foundation and the Korean Federation of Science and Technology Societies, and the Microthermal System Research Center of the Korea Science and Engineering Foundation. The authors acknowledge Wanki Min for his help in formulating part of the model.

References

[1] Ehlers, F. E., and Weatherill, W. H., "A Harmonic Analysis Method for Unsteady Transonic Flow and Its Application to the Flutter of Airfoils," NASA CR-3537, 1982.

[2] Whitehead, D. S., "Force and Moment Coefficients for Vibrating Airfoils in Cascade," British Aeronautical Research Council, Reports and Memoranda No. 3254, London, 1960.

[3] Whitehead, D. S., "Classical Two-Dimensional Methods," *AGARD Manual on Aeroelasticity in Axial Flow Turbomachines. Vol. 1: Unsteady Turbomachinery Aerodynamics*, edited by M. F. Platzer, and F. O. Carta, AGARD, Neuilly-sur-Seine, France, AGARD-AG-298, Vol. 1, March 1987, Chap. 3.

[4] Edwards, J. W., Ashley, H., and Breakwell, J. V., "Unsteady Aerodynamic Modeling for Arbitrary Motions," *AIAA Journal*, Vol. 17, No. 4, 1979, pp. 365–374.
[5] Dinyavari, M. A. H., and Friedmann, P. P., "Application of Time-Domain Unsteady Aerodynamics to Rotary-Wing Aeroelasticity," *AIAA Journal*, Vol. 24, No. 9, 1986, pp. 1424–1432.
[6] Hall, K. C., "Eigenanalysis of Unsteady Flows about Airfoils, Cascades, and Wings," *AIAA Journal*, Vol. 32, No. 12, 1994, pp. 2426–2432.
[7] Kim, T. H., Nam, C. H., and Kim, Y. D., "Reduced-Order Aeroservoelastic Model with an Unsteady Aerodynamic Eigenformulation," *AIAA Journal*, Vol. 35, No. 6, 1997, pp. 1087, 1088.
[8] Theodorsen, T., "General Theory of Aerodynamic Instability and the Mechanism of Flutter," National Advisory Committee for Aeronautics Report No. 496, 1935.
[9] Sears, W. R., "Operational Methods in a Theory of Airfoils in Non-Uniform Motion," *Journal of the Franklin Institute*, Vol. 230, No. 1, 1940, pp. 95–111.
[10] Isaacs, R., "Airfoil Theory for Flows of Variable Velocity," *Journal of the Aeronautical Sciences*, Vol. 12, No. 1, 1945, pp. 113–117.
[11] Greenberg, J. M., "Airfoil in Sinusoidal Motion in Pulsating Stream," National Advisory Committee for Aeronautics, Technical Notes, No. 1326, 1947.
[12] van der Wall, B. G., "The Influence of Variable Flow Velocity on Unsteady Airfoil Behavior," M.S. Thesis, Univ. of Maryland, College Park, MD, 1991.
[13] van der Wall, B. G., and Leishman, J. G., "On the Influence of Time-Varying Flow Velocity on Unsteady Aerodynamics," *Journal of the American Helicopter Society*, Vol. 39, No. 4, 1994, pp. 25–36.
[14] Peters, D. A., Barwey, D., and Johnson, M. J., "Finite-State Airloads Model with Compressibility and Unsteady Free-Stream," *Sixth International Workshop on Dynamics and Aeroelastic Stability Modeling of Rotorcraft Systems*, U.S. Army Research Office, 1995.
[15] Peters, D. A., Hsieh, M. A., and Torrero, A., "A State-Space Airloads Theory for Flexible Airfoils," *Proceedings of the 62nd Annual National Forum of the American Helicopter Society*, American Helicopter Society, Alexandria, VA, 2006, pp. 1806–1823.
[16] Dugundji, J., and Bundas, D. J., "Flutter and Forced Response of Mistuned Roters Using Standing Wave Analysis," *AIAA Journal*, Vol. 22, No. 11, 1984, pp. 1652–1661.
[17] Katz, J., and Plotkin, A., *Low-Speed Aerodynamics*, 2nd ed., Cambridge Univ. Press, Cambridge, England, U.K., 2001.
[18] Kim, T., Methods of Aeroservoelastic Formulation: Industrial Practices, *The 46th AIAA/ASME/ASCE/AHS/ASC Structures, Structural Dynamics and Materials Conference*, AIAA, Washington, DC, 2005.
[19] Sissingh, G. J., "Dynamics of Rotors Operating at High Advance Ratios," *Journal of the American Helicopter Society*, Vol. 13, No. 3, 1968, pp. 56–63.
[20] Peters, D. A., and Hohenemser, K. H., "Application of the Floquet Transition Matrix to Problems of Lifting Rotor Stability," *Journal of the American Helicopter Society*, Vol. 16, No. 2, 1971, pp. 25–33.
[21] Bisplinghoff, R. L., Ashley, H., and Halfman, R. L., *Aeroelasticity*, 1st ed., Dover, New York, 1996.
[22] Bolotin, V. V., *The Dynamic Stability of Elastic Systems*, Holden-Day, San Francisco, 1964.

E. Livne
Associate Editor